Rapid Communications

Theory of spin transport through an antiferromagnetic insulator

Gen Tatara and Christian Ortiz Pauyac
RIKEN Center for Emergent Matter Science (CEMS) and RIKEN Cluster for Pioneering Research (CPR), 2-1 Hirosawa, Wako, Saitama 351-0198, Japan

(Received 17 March 2019; published 9 May 2019)

A theoretical formulation for spin transport through an antiferromagnetic (AF) insulator is presented in a case that is driven/detected by the direct/inverse spin Hall effect in two heavy-metal contacts. The spin signal is shown to be transferred by the ferromagnetic correlation function of the antiferromagnet, which is calculated based on a magnon representation. To cover the high-temperature regimes, we include an auxiliary field representing short AF correlations and a temperature-dependent damping due to magnon scattering. The diffusion length for spin is long, close to the degeneracy of the two AF magnons, and has a maximum as a function of temperature near the Néel transition.

DOI: 10.1103/PhysRevB.99.180405

Spin current injection to various materials has been a crucial issue in spintronics. Of particular recent interest is spin current propagation in antiferromagnetic insulators (AFIs). Being a common material, AFIs have practical advantages in the choice of materials. Moreover, insertion of an antiferromagnetic (AF) layer between a ferromagnet and normal metal was found to enhance spin current injection efficiency [1,2]. Experimentally, spin current injection and propagation efficiency in AF insulators is reported to vanish or to be very small at $T = 0$, and to have a peak near the Néel transition temperature T_N, reducing at higher temperatures [2,3].

The transmission of spin information in antiferromagnets is an intriguing issue as fundamental science. To describe spin current injection in antiferromagnets, two issues need to be clarified, namely, to what degree of freedom the incident spin current couples, and how it propagates. Obviously, rigid AF order does not react to spin current injection having a particular spin polarization, and fluctuation is essential. There are two branches of AF magnons, corresponding to opposite spin angular momentum, and the coupling of the two modes is essential, as noted previously [4,5]. The amplitude and decay length of spin current propagation are expected to depend strongly on the temperature because of the Bose distribution function representing the number of AF magnon excitations. In fact, the spin current amplitude was found experimentally to have a peak near T_N, and this feature was explained based on a phenomenological theory using mixing conductance [2]. A sharp peak at T_N was predicted in another theory evaluating fluctuations around a mean-field solution in the spatially uniform case [6]. The frequency dependence of the magnon propagation length was theoretically studied in Ref. [3], although the relation between AF magnon propagation and spin current propagation remained untouched.

The objective of the present Rapid Communication is to provide a transparent formalism to describe the propagation of spin information through an AF insulator. We do not rely on the conventional spin current picture, as it is ambiguous due to the nonconservation of spin current. Moreover, introducing phenomenological parameters such as spin mixing conductance makes a straightforward understanding of the phenomena difficult. Here, we follow the linear response theory for an applied electric field by treating the exchange interaction between spins in heavy metals and antiferromagnets perturbatively. The description is an application of Ref. [7], indicating that spin current propagation is equivalent to the correlation function of ferromagnetic (FM) spin fluctuation or magnetic susceptibility. The ferromagnetic fluctuation of antiferromagnets is represented by an exchange or pair creation/annihilation of two AF magnons. The spin information is therefore transferred by a magnon pair correlation propagator, just in the same manner as the magnetic susceptibility in FM metals is represented by electron-hole pair propagation. The mismatch of frequencies of the FM excitation of GHz and of the AF one of THz therefore does not matter as the magnon pair correlation can absolve or emit low external frequencies. Moreover, shortening the AF correlation at high temperatures does not necessarily block spin current propagation, because, on the contrary, the FM fluctuation grows. Instead, the magnon lifetime at high temperatures is greatly reduced by strong magnon scattering [8], resulting in a significant reduction of spin current propagation. As a result, the propagation efficiency has a peak near T_N, although the peak position, determined by the competition between the fluctuation and damping, does not necessarily coincide with T_N.

The correlation of spin transport with magnetic correlation has been pointed out experimentally in Refs. [2,9,10]. In the case of spin pumping into a heavy metal, the efficiency of spin current injection was argued to be determined by the imaginary part of the magnetic susceptibility of a heavy metal divided by an external angular frequency [11], although their treatment of the external angular frequency was theoretically not comprehensive

Let us develop step by step a linear response theory to describe the nonlocal direct and inverse spin Hall effects separated by an AFI (Fig. 1) [12]. The key interaction is the coupling between heavy metals (HMs) and AFI at the interfaces. Here, we consider an *sd* exchange interaction between electron spin polarization in the HM and FM components of

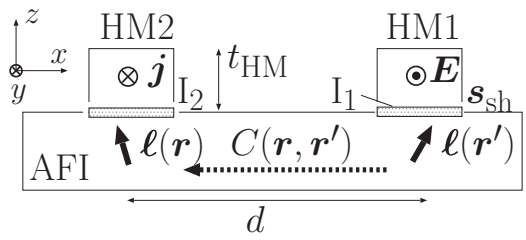

FIG. 1. Setup of nonlocal direct and inverse spin Hall effects. HM1 and HM2 are heavy-metal leads for spin current generation and detection, respectively. In the conventional picture, "spin current" generated by the spin Hall effect in HM1 is transmitted through AFI and measured at HM2 by the inverse spin Hall effect. The coupling between HM1 and HM2 at interfaces I_1 and I_2, respectively, is induced by the interface exchange interaction J_I between the spin polarization in HMs and FM spin component $\boldsymbol{\ell}$ of AFI. "Spin current propagation" through AFI is expressed by the FM correlation function $C(\boldsymbol{r},\boldsymbol{r}')$ of $\boldsymbol{\ell}$. The moment $\boldsymbol{\ell}$ is related to the Néel vector $\boldsymbol{n}$ as $\boldsymbol{\ell} \propto \boldsymbol{n} \times \dot{\boldsymbol{n}}$, and it turns out that spin information is transferred only if $\boldsymbol{n} \parallel \hat{\boldsymbol{x}}$ in the present geometry.

AFI, namely,

$$H_{\rm I} = \sum_{i=1,2} J_{\rm I} \int_{I_i} \frac{d^3r}{a^3} \boldsymbol{\ell} \cdot (c^\dagger \boldsymbol{\sigma} c), \tag{1}$$

where I_i $(i = 1, 2)$ denotes the interface between HMi and AFI, $J_{\rm I}$ is a coupling strength, $\boldsymbol{\sigma}$ denotes the Pauli matrix, and $c^\dagger$ and c are electron field operators. The FM moment of AFI is defined as $\boldsymbol{\ell} \equiv (\boldsymbol{S}_{\rm A} + \boldsymbol{S}_{\rm B})/S$, where $\boldsymbol{S}_{\rm A}$ and $\boldsymbol{S}_{\rm B}$ are spins on the two sublattices A and B, respectively ($S \equiv |\boldsymbol{S}_{\rm A}| = |\boldsymbol{S}_{\rm B}|$). This coupling is natural as the first approximation as the electron wave-function overlap would smear out the staggered (Néel) component of localized spin in AFI. Coupling of the spin accumulation to the uncompensated Néel vector as discussed for the case of spin pumping in Ref. [5] is not taken into account in the present study.

Let us start with the inverse spin Hall effect (ISHE) in HM2. In the context of linear response theory, the driving field of ISHE is a nonequilibrium FM moment $\boldsymbol{\ell}$ of AFI in Eq. (1). The output electric current is thus described by a correlation function of current and spin density $\tilde{\chi}^{JS}_{ik}$ as $j_i = J_{\rm I} \tilde{\chi}^{JS}_{ik} \ell_k$ (suppressing spatial coordinates). (The exact expression is presented in Ref. [12].) The FM moment $\boldsymbol{\ell}$ near I_2 is generated nonlocally by the spin Hall effect (SHE) in HM1. The SHE is described by the correlation function $\tilde{\chi}^{SJ}$, the reciprocal of $\tilde{\chi}^{JS}$, as $s_{{\rm sh},l} = \tilde{\chi}^{SJ}_{lj} E_j$, where $s_{{\rm sh},l}$ and E_j are the spin density induced by SHE and the applied electric field in HM1, respectively [7]. Taking account of $H_{\rm I}$, the FM moment $\boldsymbol{\ell}$ induced near I_2 by the spin accumulation at I_1 as a result of SHE is written using the nonlocal FM spin correlation function $C(\boldsymbol{r})$ as $\ell_k(\boldsymbol{r}_1) = J_{\rm I} \int_{I_2} d^3r_2 C_{kl}(\boldsymbol{r}_1 - \boldsymbol{r}_2) \tilde{\chi}^{SJ}_{lj}(\boldsymbol{r}_2) E_j(\boldsymbol{r}_2)$, where subscripts k and l denote the spin direction. As the FM moment is expressed as a composite field of two AF magnons, the correlation function $C(\boldsymbol{r})$ is a two-magnon propagator, as we shall see below.

Summarizing, the inverse spin Hall current is represented as a product of three correlation functions as

$$j_i(\boldsymbol{r}) = (J_I)^2 \int_{I_1} d^3r_1 \int_{I_2} d^3r_2 \int_{\rm HM1} d^3r' \tilde{\chi}^{JS}_{ij}(\boldsymbol{r} - \boldsymbol{r}_2) \times C_{kl}(\boldsymbol{r}_2 - \boldsymbol{r}_1) \tilde{\chi}^{SJ}_{lm}(\boldsymbol{r}_1 - \boldsymbol{r}') E_m(\boldsymbol{r}'). \tag{2}$$

The correlation functions in Eq. (2) turn out to be the physical correlation function χ^{JS} determined by the lesser component divided by the external frequency Ω, i.e., $\tilde{\chi}^{JS}_{ij} \equiv -\lim_{\Omega\to 0} \frac{1}{i\Omega} \chi^{JS}_{ij}(\Omega)$ [12]. The correlation function χ^{JS} is linear in Ω because the equilibrium spin accumulation does not generate an electric current that is dissipative, and thus $\tilde{\chi}^{JS}$ has a static component. Moreover, considering HM as a bulk, inversion symmetry is present and the spatially uniform component of the current-spin correlation vanishes, meaning that χ^{JS}_{ij} starts from the first order in the external wave vector $\boldsymbol{q}$ [7]. Thus, direct and inverse spin Hall effects with current perpendicular to the spin accumulation profile are described in the ballistic case by the correlation function $\tilde{\chi}^{JS}_{ij}(\boldsymbol{q}, \Omega) = i\lambda_{\rm sh} \epsilon_{ijk} q_k$, where ϵ_{ijk} is the totally antisymmetric tensor. A coefficient $\lambda_{\rm sh}$, determined by the spin-orbit interaction strength, is related to the dimensionless spin Hall angle $\theta_{\rm sh} (\equiv j_s/j)$ as $\theta_{\rm sh} = \lambda_{\rm sh}/(\sigma_B \tau_e)$, where σ_B and τ_e are the Boltzmann conductivity and elastic electron lifetime, respectively [7]. Taking account of the diffusive electron motion in HMs, the function is multiplied by a diffusion factor $D_{\rm s}(\boldsymbol{q}) \equiv \frac{1}{Dq^2\tau + \gamma_{\rm sf}}$, where D is a diffusion constant, $\gamma_{\rm sf}$ is related to a static spin diffusion length $\ell_{\rm sf}$ in HM as $\ell_{\rm sf} = \sqrt{3}\ell_e/\sqrt{\gamma_{\rm sf}}$, $\ell_e = k_F \tau_e/m$ being the electron elastic mean free path, as [7]

$$\tilde{\chi}^{JS}_{ij}(\boldsymbol{q}) = \lambda_{\rm sh} \epsilon_{ijk} i q_k D_{\rm s}(q). \tag{3}$$

The current is therefore expressed as

$$j_i(\boldsymbol{r}) = (\lambda_{\rm sh} J_I)^2 \epsilon_{ijk} \epsilon_{lmn} \int_{I_1} d^3r_1 \int_{I_2} d^3r_2 \nabla^r_j D_{\rm s}(\boldsymbol{r} - \boldsymbol{r}_2) \times \int_{\rm HM1} d^3r' C_{kl}(\boldsymbol{r}_2 - \boldsymbol{r}_1) \nabla^{r'}_m D_{\rm s}(\boldsymbol{r}_1 - \boldsymbol{r}') E_n(\boldsymbol{r}'), \tag{4}$$

where the spin diffusion propagator is $D_{\rm s}(\boldsymbol{r}) = \frac{3\ell_{\rm sf} a_0}{2\ell_e{}^2} e^{-\frac{r}{\ell_{\rm sf}}}$ (a_0 is the lattice constant of HM). The spatial derivative of spin diffusions in Eq. (4) represents the spin current flow of the conventional picture, as the spin current is proportional to a gradient of spin density in the diffusive regime. In the common setup in Fig. 1, the derivatives are in the perpendicular direction, which we choose as the z direction. The derivative at I_1 of HM1 is evaluated as $\nabla_z D_{\rm s}|_{r=0} = -\frac{3a_0}{2\ell_e{}^2}$. For HM2, we discuss the averaged current for the thickness of HM2, $t_{\rm HM}$, i.e., $\bar{j} \equiv \frac{1}{t_{\rm HM}} \int_0^{t_{\rm HM}} dz j(z)$, where we use $\frac{1}{t_{\rm HM}} \int_0^{t_{\rm HM}} dz \nabla_z D_{\rm s}(z) = -\frac{3\ell_{\rm sf} a_0}{2t_{\rm HM}\ell_e{}^2}(1 - e^{-t_{\rm HM}/\ell_{\rm sf}})$.

The correlation function of AFI, C_{kl}, is calculated later and we proceed here using the results. It turns out to vanish for the spin direction perpendicular to the Néel vector $\boldsymbol{n}$, and the spatial dependence is exponential in most cases. We denote the direction in the spin space of AFI as (1, 2, 3) to remember that spin space is independent of the coordinate space, and $\boldsymbol{n}$ is chosen along the 3-direction. As shown below, the correlation

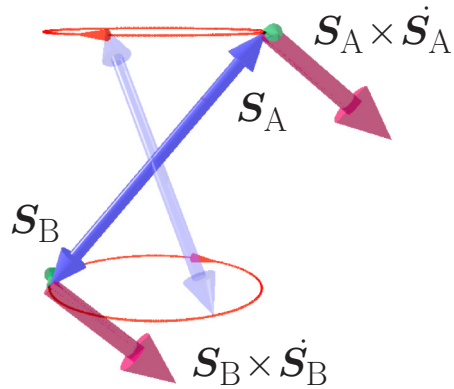

FIG. 2. Schematic picture showing that the FM moment ℓ is proportional to $\boldsymbol{n}\times\dot{\boldsymbol{n}}$. For both sublattices A and B with opposite spin, $\boldsymbol{S}_\mathrm{A}\simeq S\boldsymbol{n}$ and $\boldsymbol{S}_\mathrm{B}\simeq -S\boldsymbol{n}$, $\boldsymbol{S}_\mathrm{A}\times\dot{\boldsymbol{S}}_\mathrm{A}$ and $\boldsymbol{S}_\mathrm{B}\times\dot{\boldsymbol{S}}_\mathrm{B}$ (large arrows) point in the same direction.

function of AFI is $C_{kl}=\delta_{k3}\delta_{l3}C(\boldsymbol{r})$, where

$$C(\boldsymbol{r})=c_0\frac{a}{2\xi}e^{-|\boldsymbol{r}|/\xi}, \tag{5}$$

with a dimensionless constant c_0 and a FM correlation length ξ (a is the lattice constant of AFI). Choosing the applied current direction as the y axis (Fig. 1), the antisymmetric tensors in Eq. (4) indicate that "spin current" propagates only if $\boldsymbol{n}(=\hat{\boldsymbol{3}})=\hat{\boldsymbol{x}}$.

The ISH current is opposite to the applied electric field. Defining an effective nonlocal conductivity $\overline{\sigma}$ as $\bar{j}\equiv-\overline{\sigma}E$, we have

$$\frac{\overline{\sigma}}{\sigma_B}=\frac{3}{8}(\theta_\mathrm{sh})^2(J_I)^2\nu\tau\left(\frac{a_0}{\ell_e}\right)^2\frac{c_0a}{\xi}e^{-d/\xi}\frac{\ell_\mathrm{s}}{t_\mathrm{HM}}(1-e^{-t_\mathrm{HM}/\ell_\mathrm{s}}), \tag{6}$$

where d is the distance between HM1 and HM2, and ν is the electron density of states. The electron properties are insensitive to the temperature around room or lower temperatures. According to the analysis below, the ratio $\frac{c_0a}{\xi}$ of AFI does not depend much on the temperature either, as both c_0 and ξ have similar temperature profiles [Fig. 3(b)], and thus the dominant temperature dependence is expected to arise from $e^{-d/\xi(T)}$. Equation (6) indicates that the interface exchange coupling constant J_I can be determined experimentally from the magnitude of ISHE.

Let us start a study of the correlation in AFI. We first note that the FM moment is expressed by $\boldsymbol{n}$ as $\boldsymbol{\ell}=\frac{1}{6SJ_0}(\boldsymbol{n}\times\dot{\boldsymbol{n}})$, where J_0 is the AF exchange coupling. This relation, rigorously derived in Ref. [12], is understood by noting that $\boldsymbol{S}\times\dot{\boldsymbol{S}}$ points in the same direction for the spins of both sublattices A and B (Fig. 2). The Néel vector has a classical expectation value n_3 along the direction $\hat{\boldsymbol{3}}$ below the AF transition temperature T_N. The fluctuation is represented by a two-component AF magnon field $\boldsymbol{\varphi}$ as $\boldsymbol{n}=(\varphi^{(1)},\varphi^{(2)},n_3)$, neglecting the second order of the magnon field. The FM moment around $\boldsymbol{n}$ is therefore represented by a combination of the two magnons as $\ell_3=\varphi^{(1)}\dot{\varphi}^{(2)}-\dot{\varphi}^{(1)}\varphi^{(2)}$, while the orthogonal components are linear in the magnon field. Considering the fact that AF dynamics (typically in the THz regime) is much faster than the FM one (GHz), only the moment ℓ_3 has a low-energy coupling to AF magnons. Namely, the spin polarization parallel to $\boldsymbol{n}$ can be transported for a long distance, while AFI does not react to the perpendicular polarization, resulting in $C_{kl}(\boldsymbol{q})\equiv\delta_{k3}\delta_{l3}C_{\boldsymbol{q}}$. This feature is in agreement with a recent experiment [13]. The two magnon modes $\varphi^{(1)}$ and $\varphi^{(2)}$ carry opposite angular momentum, and thus the FM moment is induced by an exchange of the two modes (ordinary process) or by a pair annihilation or creation (anomalous processes). In terms of magnon creation/annihilation operators $a^{(i)}$ and $a^{(i)\dagger}$ ($i=1,2$), introduced as $\varphi_i(k)=\sqrt{\frac{g}{\omega_k^{(i)}}}(a_k^{(i)}+a_{-k}^{(i)\dagger})$ ($g=3J_0$), the expectation value of the induced moment with wave vector $\boldsymbol{q}$ reads

$$\begin{aligned}\langle\ell_3(\boldsymbol{q},t)\rangle=\frac{1}{2S}\sum_{\boldsymbol{k}}\frac{1}{\sqrt{\omega_{\boldsymbol{k}}^{(1)}\omega_{\boldsymbol{k}+\boldsymbol{q}}^{(2)}}}\Big[&\big(\omega_{\boldsymbol{k}+\boldsymbol{q}}^{(2)}-\omega_{\boldsymbol{k}}^{(1)}\big)[F_{-\boldsymbol{k},\boldsymbol{k}+\boldsymbol{q}}(t,t)\\&-\overline{F}_{\boldsymbol{k},-(\boldsymbol{k}+\boldsymbol{q})}(t,t)]+\big(\omega_{\boldsymbol{k}+\boldsymbol{q}}^{(2)}+\omega_{\boldsymbol{k}}^{(1)}\big)\big[D_{\boldsymbol{k}+\boldsymbol{q},\boldsymbol{k}}^{(21)}(t,t)\\&-D_{-\boldsymbol{k},-(\boldsymbol{k}+\boldsymbol{q})}^{(12)}(t,t)\big]\Big],\end{aligned} \tag{7}$$

where $\omega_{\boldsymbol{k}}^{(i)}\equiv\sqrt{(v\boldsymbol{k})^2+(\Delta^{(i)})^2}$ is the magnon energy for branch i (v and $\Delta^{(i)}$ being the magnon velocity and gap, respectively) and

$$\begin{aligned}F_{-\boldsymbol{k},\boldsymbol{k}+\boldsymbol{q}}(t,t')&\equiv-i\big\langle a_{-\boldsymbol{k}}^{(1)}(t)a_{\boldsymbol{k}+\boldsymbol{q}}^{(2)}(t')\big\rangle,\\D_{\boldsymbol{k}+\boldsymbol{q},\boldsymbol{k}}^{(ij)}(t,t')&\equiv-i\big\langle a_{\boldsymbol{k}+\boldsymbol{q}}^{(i)}(t)a_{\boldsymbol{k}}^{(j)\dagger}(t')\big\rangle,\end{aligned} \tag{8}$$

are anomalous and ordinary path-ordered Green's functions on a complex time path and $\overline{F}\equiv F^*$. The static component of $\langle\ell_3\rangle$ induced by SHE in HM1 is written using a correlation function $C_{\boldsymbol{q}}$ as $\langle\ell_3(\boldsymbol{q})\rangle\equiv J_\mathrm{I}C_{\boldsymbol{q}}s_{\mathrm{sh},3}(\boldsymbol{q})$, where

$$C_{\boldsymbol{q}}=\frac{g}{2S}\sum_{\boldsymbol{k}}\mathrm{Re}\left[\frac{1}{\omega_{\boldsymbol{k}}^{(1)}\omega_{\boldsymbol{k}+\boldsymbol{q}}^{(2)}}\left(\big(1+n_{\boldsymbol{k}}^{(1)}+n_{\boldsymbol{k}+\boldsymbol{q}}^{(2)}\big)\frac{\big(\omega_{\boldsymbol{k}+\boldsymbol{q}}^{(2)}-\omega_{\boldsymbol{k}}^{(1)}\big)^2}{\omega_{\boldsymbol{k}+\boldsymbol{q}}^{(2)}+\omega_{\boldsymbol{k}}^{(1)}-i(\eta_{\boldsymbol{k}}+\eta_{\boldsymbol{k}+\boldsymbol{q}})}-\big(n_{\boldsymbol{k}+\boldsymbol{q}}^{(2)}-n_{\boldsymbol{k}}^{(1)}\big)\frac{\big(\omega_{\boldsymbol{k}+\boldsymbol{q}}^{(2)}+\omega_{\boldsymbol{k}}^{(1)}\big)^2}{\omega_{\boldsymbol{k}+\boldsymbol{q}}^{(2)}-\omega_{\boldsymbol{k}}^{(1)}-i(\eta_{\boldsymbol{k}}+\eta_{\boldsymbol{k}+\boldsymbol{q}})}\right)\right]. \tag{9}$$

Here, $n_{\boldsymbol{k}}^{(i)}\equiv[e^{\beta\omega_{\boldsymbol{k}}^{(i)}}-1]^{-1}$ is Bose distribution function [$\beta\equiv1/(k_BT)$, k_B being the Boltzmann constant], $\eta_{\boldsymbol{k}}$ represents magnon damping, and Re denotes the real part. The first term of the right-hand side of Eq. (9) without a Bose distribution function is the quantum contribution that exists at $T=0$. Spin current can thus transmit though the antiferromagnet at $T=0$, where no magnons are excited. (The quantum pair creation process has been shown to be essential for the neutron scattering of Haldane antiferromagnets at $T=0$ [14].)

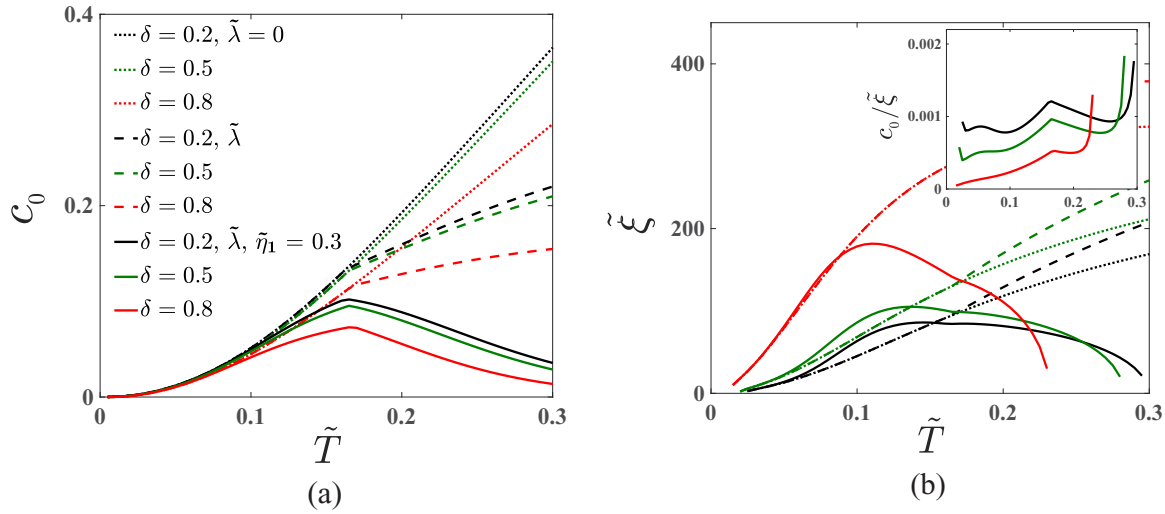

FIG. 3. Plots of (a) c_0 and (b) dimensionless FM correlation length $\tilde{\xi} \equiv \xi/a$ as functions of normalized temperature, $\tilde{T} \equiv k_B T/\omega_{\max}$, where $\omega_{\max} \equiv v k_{\max}$ is the maximum magnon energy, $k_{\max} \equiv \pi/a$. Dotted lines are without an auxiliary field $\lambda(\equiv \tilde{\lambda}\omega_{\max}^2)$ and for $\eta_1 = 0$, the dashed lines are with λ and for $\eta_1 = 0$, and solid lines are physical ones including both λ and $\tilde{\eta}_1 \equiv \eta_1/\omega_{\max} = 0.3$. Bare damping is $\eta_0/\omega_{\max} = 10^{-4}$, and the two energy gaps are Δ and $\Delta\delta$, with $\Delta/\omega_{\max} = 0.03$ and $\delta = 0.2$, 0.5, and 0.8. The Néel temperature in the present model is $\tilde{T}_N \simeq 0.16$. The inset of (b) shows the ratio $\frac{c_0}{\tilde{\xi}}$, which governs the amplitude of the ISH signal [Eq. (6)]. Anomalous behaviors in the high-temperature regime with $\xi \lesssim 0$ indicate the breakdown of our model.

The correlation function determines the spatial profile of steady "spin current propagation." Long-range behavior is determined by the small q behavior,

$$C_q = c_0 + c_2 q^2 + O(q^4). \tag{10}$$

For the degenerate case, $\omega_k^{(1)} = \omega_k^{(2)}$, the uniform contribution c_0 vanishes. When the two spin waves have different gaps as a result of magnetic anisotropy (as in the case of NiO), the uniform component c_0 is finite, which leads to efficient "spin current propagation." The length scale of the spin information propagation, a diffusion length of spin, is given by $\xi \equiv \sqrt{-\frac{c_2}{c_0}}$, as the response function is approximately written as $C_q \simeq \frac{c_0}{1+\xi^2 q^2} + O(q^4)$, which leads in the real space to an exponential decay within a distance of ξ, Eq. (5).

Figure 3 shows numerical results of c_0 and ξ as functions of temperature in nondegenerate cases with the two energy gaps $\Delta^{(1)} = \Delta$ and $\Delta^{(2)} = \Delta\delta$. Close to the degeneracy, $\delta \sim 1$, spin transport is long ranged (larger ξ) as the transport is mediated by the mixing of the two magnon branches. In contrast, c_0 representing the magnitude of spin transmission is suppressed for larger δ, simply due to an increase of $\Delta^{(2)}$.

Magnon representation is usually applied to low temperatures compared to T_N. However, the representation itself does not necessarily break down even above T_N as far as short-ranged AF correlation persists for a length longer than the lattice constant, just as the case of FM magnons well defined in the presence of structures such as a domain wall. A short-ranged correlation is theoretically described by introducing an auxiliary field $\lambda(T)$ to impose the constraint $|\boldsymbol{n}| = 1$ by the saddle-point approximation [15]. The field contributes to a temperature-dependent gap and modifies the magnon dispersion to be $\omega_k^{(i)} = \sqrt{v^2k^2 + (\Delta^{(i)})^2 + \lambda}$. The static AF correlation length, $\xi_{\rm AF}^{(i)} = v/\sqrt{(\Delta^{(i)})^2 + \lambda + \eta_k^2}$, including damping η_k, is usually shorter than the FM correlation length governing spin propagation (see Figs. 6 and 7 of Ref. [12]). The auxiliary field description is known to describe well the AF correlation length above T_N [15,16].

What is most essential for transport at high temperatures is the magnon damping due to magnon interactions at high densities. The effect of magnon interactions on damping was studied theoretically in detail in Ref. [8]. It was shown that the scattering induces a self-energy proportional to T^3 and ω_k^2 for low-energy magnons. We here include the effect in the damping constant η as

$$\eta(T,k) = \eta_0 + \eta_1 \left(\frac{k}{k_{\max}}\right)^2 \left(\frac{k_B T}{\omega_{\max}}\right)^3, \tag{11}$$

where η_0 and η_1 are constants, and $k_{\max} \equiv \pi/a$ and $\omega_{\max} \equiv v k_{\max}$ are the cutoffs for high wave vector and energy, respectively. The spin propagation efficiency c_0 and FM correlation length ξ are significantly suppressed by the temperature-dependent damping at high temperatures as seen in Fig. 3 (solid and dashed lines). The peak temperature, determined by the competition between the magnon excitation number and damping, is close to T_N.

Considering the case of NiO, $\omega_{\max}/(2\pi) = 30$ THz, $\Delta^{(1)} = 1$ THz, $\Delta^{(2)} = 0.2$ THz, and $a = 4.2$ Å [4], and our calculation ($\tilde{\Delta} = 0.03$, $\delta = 0.2$) indicates a spin transport length ξ of the order of 20 nm around room temperature, which appears to be roughly consistent with an experiment indicating a diffusion length of 10 nm [9]. For quantitative calculations, however, our model, assuming a square lattice with nearest-neighbor hopping, is too simple and more realistic modeling is necessary.

We have presented a theoretical formulation of spin injection into an antiferromagnetic insulator (AFI) using direct and inverse spin Hall effects. The spin current propagation,

induced by AF magnon pair propagation, was shown to be represented by a ferromagnetic (FM) correlation function C_q or a q-resolved FM susceptibility. Although C_q may appear to be similar to the conductivity for the spin current in analogy with the case of a charge current, this is not the case because a correlation function of the spin current representing the spin current conductivity cannot be written by a spin correlation as spin is not conserved. The correlation function was studied based on a magnon representation including an auxiliary field in the stationary-field approximation to cover the temperatures above the Néel temperature T_N. The decay length of spin propagation ξ was calculated from a pair propagation process for the nondegenerate case. It is different from (longer than) the AF correlation length ξ_{AF} determined by individual AF magnon propagation, similarly to the electron case where transport lengths are longer than the elastic mean free path. $\xi(T)$ has a peak near T_N as a result of suppression due to the damping arising from magnon scattering at high temperatures. The dominant temperature dependence of the spin propagation efficiency through AFI for a distance of d is thus expected to be $e^{-d/\xi(T)}$.

G.T. thanks T. Ono, E. Saitoh, R. Lebrun, and M. Kläui for valuable discussions. He is grateful for the Graduate School Materials Science in Mainz (MAINZ) for financial support (DFG GSC 266). This work was supported by a Grant-in-Aid for Exploratory Research (No. 16K13853) and a Grant-in-Aid for Scientific Research (B) (No. 17H02929) from the Japan Society for the Promotion of Science and a Grant-in-Aid for Scientific Research on Innovative Areas (No. 26103006) from The Ministry of Education, Culture, Sports, Science and Technology (MEXT), Japan.

[1] H. Wang, C. Du, P. C. Hammel, and F. Yang, Phys. Rev. Lett. **113**, 097202 (2014).
[2] W. Lin, K. Chen, S. Zhang, and C. L. Chien, Phys. Rev. Lett. **116**, 186601 (2016).
[3] J. Cramer, U. Ritzmann, B.-W. Dong, S. Jaiswal, Z. Qiu, E. Saitoh, U. Nowak, and M. Kläui, J. Phys. D **51**, 144004 (2018).
[4] S. M. Rezende, R. L. Rodríguez-Suárez, and A. Azevedo, Phys. Rev. B **93**, 054412 (2016).
[5] R. Khymyn, I. Lisenkov, V. S. Tiberkevich, A. N. Slavin, and B. A. Ivanov, Phys. Rev. B **93**, 224421 (2016).
[6] S. Okamoto, Phys. Rev. B **93**, 064421 (2016).
[7] G. Tatara, Phys. Rev. B **98**, 174422 (2018).
[8] A. B. Harris, D. Kumar, B. I. Halperin, and P. C. Hohenberg, Phys. Rev. B **3**, 961 (1971).
[9] H. Wang, C. Du, P. C. Hammel, and F. Yang, Phys. Rev. B **91**, 220410(R) (2015).
[10] Z. Qiu, J. Li, D. Hou, E. Arenholz, A. T. N'Diaye, A. Tan, K.-i. Uchida, K. Sato, S. Okamoto, Y. Tserkovnyak, Z. Q. Qiu, and E. Saitoh, Nat. Commun. **7**, 12670 (2016).
[11] Y. Ohnuma, H. Adachi, E. Saitoh, and S. Maekawa, Phys. Rev. B **89**, 174417 (2014).
[12] See Supplemental Material at http://link.aps.org/supplemental/10.1103/PhysRevB.99.180405 for a mathematical derivation and details of the magnon transport properties.
[13] R. Lebrun, A. Ross, S. A. Bender, A. Qaiumzadeh, L. Baldrati, J. Cramer, A. Brataas, R. A. Duine, and M. Kläui, Nature (London) **561**, 222 (2018).
[14] I. Affleck and R. A. Weston, Phys. Rev. B **45**, 4667 (1992).
[15] S. Chakravarty, B. I. Halperin, and D. R. Nelson, Phys. Rev. B **39**, 2344 (1989).
[16] H. Yamamoto, G. Tatara, I. Ichinose, and T. Matsui, Phys. Rev. B **44**, 7654 (1991).